# Determination of the phase boundary between the *B*1 and *B*2 phases in NaCl by *in situ* x-ray diffraction

Norimasa Nishiyama,[1,*] Tomoo Katsura,[2] Ken-ichi Funakoshi,[3] Atsushi Kubo,[2] Tomoaki Kubo,[4] Yoshinori Tange,[5] Yu-ichiro Sueda,[1] and Sho Yokoshi[2]

[1]*Geodynamics Research Center, Ehime University, 2-5 Bunkyo-cho, Matsuyama 790-8577, Japan*

[2]*Institute for Study of the Earth's Interior, Okayama University, Misasa, Touhaku-gun, Tottori 628-0193, Japan*

[3]*Japan Synchrotron Radiation Research Institute, Mikazuki, Sayo-gun, Hyogo 679-5198, Japan*

[4]*Department of Mineralogy, Petrology, and Economic Geology, Tohoku University, Sendai 980-8578, Japan*

[5]*Department of Earth and Planetary Sciences, Tokyo Institute of Technology, Meguro 152-8550, Japan*

(Received 13 May 2003; published 17 October 2003)

The equilibrium phase boundary between the *B*1 and *B*2 phases in NaCl was determined at temperatures between 1150 and 2000 K by *in situ* x-ray diffraction, using a Kawai-type apparatus in a beam line of SPring-8, Hyogo, Japan. The press was oscillated during data acquisition in order to reduce the effect of grain growth on the diffraction pattern of NaCl at high temperature, obtained by the energy-dispersive method with a fixed angle. Forward (*B*1 to *B*2) and backward (*B*2 to *B*1) transitions were observed independently at temperatures between 1150 and 1600 K; the *P*-*T* conditions where these transitions occur fall on a straight line, indicating that there is no kinetic effect between the forward and the backward transitions over this temperature range. The equilibrium phase boundary is represented by the linear equation $P$ (in GPa) $= 30.6(2) - 0.0053(2)\ T$ (in K). Liquid NaCl was observed at 20.1 GPa and 2100 K, consistent with the melting curve obtained in a previous study using a laser- heated diamond anvil cell. According to our experimental results, the triple point between *B*1, *B*2, and liquid NaCl would be located at $19.7 \pm 0.5$ GPa and $2050 \pm 50$ K.

DOI: 10.1103/PhysRevB.68.134109 PACS number(s): 64.70.Kb, 61.10.Nz

## I. INTRODUCTION

NaCl is one of the simplest and most thoroughly studied ionic crystals. Thus, physical properties of NaCl such as its phase transformation, compressibility, and thermal expansivity can provide a basic model for understanding the physical properties of more complex ionic crystals. It has been well established that NaCl with the rocksalt structure (the *B*1 phase) transforms into the CsCl structure (the *B*2 phase) at about 30 GPa and room temperature.[1–3] However, transition pressures at high temperatures have not yet been well established nor well-studied experimentally. The accurate location of this phase boundary in *P*-*T* space is useful for x-ray diffraction experiments at high pressure and temperature because the *B*1 phase is frequently used as a pressure calibrant. The *B*1 phase of NaCl is one of the best pressure calibrants because it is very compressible [$K_{300,0} \sim 24$ GPa (Ref. 4)] and its *P*-*V*-*T* equation of state has been well established.[4–6] But in *P*-*T* conditions above this phase boundary, NaCl is unusable as a pressure calibrant because of its transformation to the *B*2 phase. Thus, this phase boundary sets a limit to the *P*-*T* conditions where the *B*1 phase can be used as a pressure calibrant.

Pioneering studies of this transformation at high temperatures employed shock wave (Hugoniot) measurements of NaCl.[7,8] In these studies, the *B*1 to *B*2 transition was observed at around 24 GPa and 1000 K, which demonstrated that the Clapeyron slope of this phase boundary must be negative. Li and Jeanloz[9] studied this phase boundary using an externally heated diamond anvil cell, and the maximum temperature of their experiment was limited to 673 K. They judged the stable phase at a given *P*-*T* conditions by the visual observation on the basis of the difference in refractive indices of the two phases. Boehler, Ross, and Boercker[10] have developed experimental techniques to measure melting temperatures using a laser-heated diamond anvil cell, and have performed experiments to measure the melting temperature of NaCl at pressures up to 91 GPa. They observed a discontinuous change in the NaCl melting curve of NaCl at about 29 GPa and 2300 K, which they interpreted as originating from the triple point among *B*1, *B*2, and liquid. Since the maximum temperature of the Li- Jeanloz study is 673 K, there is no experimental data for the *B*1-*B*2 transition pressure between 673 K and the melting temperature by a static high-pressure study.

In order to elucidate the phase boundary between *B*1 and *B*2 phases of NaCl at high temperatures, we carried out a series of x-ray diffraction experiments at high pressure and temperature on NaCl using a Kawai-type apparatus. In order to determine a phase boundary in *P*-*T* space, the *in situ* x-ray observation is the most essential technique because stable structures are determined directly at high *P*-*T* conditions. In addition, a Kawai-type apparatus with an internal resistance heater can generate high temperatures up to 2500 K with a small temperature fluctuation (less than $\pm 5$ K), at pressures up to 30 GPa. Therefore, a combination of a Kawai-type apparatus and synchrotron radiation for the *in situ* x-ray diffraction study is the most suitable technique to determine the *B*1-*B*2 phase boundary in NaCl. In addition, special attention was paid to phase identification in NaCl at high pressure and temperature. The press was oscillated during data acquisition in order to reduce the effect of NaCl grain growth at high temperatures on the diffraction patterns. In this paper, we report experimental data on this phase boundary at tem-

 

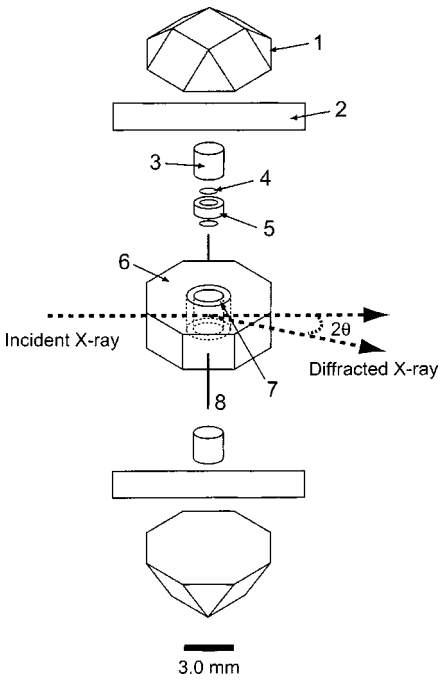


FIG. 1. A schematic illustration of the cell assembly for TEL = 3.0 mm used in the present study: 1, pressure medium (MgO); 2, electrode (Mo); 3, $ZrO_2$ rod; 4, rhenium disk; 5, sample container (graphite); 6, pressure medium ($ZrO_2$), 7, heater ($LaCrO_3$); 8, thermocouple ($W_{97}Re_3$-$W_{75}Re_{25}$).

peratures up to 2100 K, including melting of NaCl at about 20 GPa.

## II. EXPERIMENTAL PROCEDURE

The *in situ* x-ray diffraction experiment was performed in the beam line BL04B1, SPring-8. Since 2002, a newly constructed Kawai-type apparatus named SPEED-Mk.II and a system for energy-dispersive x-ray diffraction measurements have been installed in this beam line.[10] Incident x rays from a bending magnet were collimated to form a thin beam (50 $\mu$m in horizontal and 200 $\mu$m in vertical dimensions) using tungsten carbide slits; this beam was directed to the sample chamber after passing through pyrophyllite gaskets and pressure media (Fig. 1). Diffracted x rays were detected by a pure Ge solid-state detector and a 4096-channel analyzer situated at a fixed diffraction angle of about 6°, after passing through a collimator with a 50-$\mu$m horizontal slit and additional tungsten carbide slits (200 $\mu$m in horizontal and 500 $\mu$m in vertical dimensions). The exact diffraction angle was calibrated using *d* values of x-ray diffraction peaks for NaCl and MgO, which was used as an internal pressure marker, at ambient conditions.

This Kawai-type apparatus consists of a 15 MN hydraulic press with a newly designed DIA-type guide block to squeeze an inner anvil assembly, which is composed of eight cube-shaped tungsten carbide (WC) anvils with truncated corners.[11] The truncated edge length (TEL) of the inner WC anvils is 3.0 mm. The truncated corners of the eight anvils make an octahedral cavity for the cell assembly.

Figure 1 shows the schematic illustration of a cell assembly used in the present study. In order to minimize temperature fluctuation at high temperature and to carry out high *P-T* experiments with long run duration (over 24 h), a cylindrical lanthanum chromite heater with two graphite windows for passage of the incident and diffracted x-ray beam was used. Upper and lower parts of the pressure media were made of semisintered magnesia, and semisintered zirconia was used as the central part of the pressure media, which also serves as a thermal insulator. Two MgO rods were embedded in the center of the zirconia for passage of x rays.

The sample chamber consisted of a graphite tube (0.8 mm ID, 1.4 mm OD, and 0.5 mm in height) covered with two rhenium disks (0.8 mm in diameter and 0.025 mm in thickness), which separate the sample from the surrounding materials and also promote a homogeneous temperature distribution within the sample. This sample chamber transformed to diamond at high pressure and temperature within the experimental conditions of 20–25 GPa and 1000–2000 K. The diamond sample chamber is suitable for *in situ* x-ray diffraction experiments because of its high transparency to x rays and high thermal conductivity, which achieves a uniform temperature distribution within the sample, and because it does not react with the sample and heater.

The sample consisted of a mixture of NaCl (99.9% purity, Kanto Kagaku) and MgO with a 1:1 ratio in volume. MgO was used as an internal pressure marker and also serves to inhibit rapid grain growth of NaCl at high temperature. The temperature was measured by a $W_{0.97}Re_{0.03}$–$W_{0.75}Re_{0.25}$ thermocouple, without corrections for the effect of pressure on thermocouple emf.

The cell assembly was first compressed to the maximum load of 15 MN, and then temperature was slowly increased. As temperature was increased, x-ray diffraction patterns of the sample were obtained in order to identify which phase of NaCl was present. Once the *B*2 phase was observed, the press load and/or temperature was changed in order to identify the stable phase at a different *P-T* condition. At temperatures above 1100 K, the press was oscillated within an angular range from −4° to 7° during data acquisition. To our knowledge, this is the first press with an oscillation system.[11] A problem that sometimes occurs in x-ray diffraction experiments at high pressure and temperature using the energy-dispersive method with fixed angle is that minor peaks of a given sample have greater intensity than its major peaks, and sometimes the major peaks disappear altogether.[11,12] These unusual relative intensities in the diffraction peaks of the sample are attributable to a shortage in the number of grains contributing to the x-ray diffraction patterns, because grain growth occurs in the sample at high temperature. This problem prevents us from accurately identifying the phase present in the sample in experiments whose objective is to define the position of a phase boundary by *in situ* x-ray diffraction, and prevents us from determining lattice volumes accurately at high pressure and temperature in experiments designed to determine a *P-V-T* equation of state. In order to solve this problem, the SPEED-Mk. II press was constructed with an oscillation system, the usefulness of which has already been confirmed by x-ray diffraction patterns collected on a sample with a small number of grains at high

temperature.[11] In the present study, all the x-ray diffraction patterns above 1100 K were acquired using this press-oscillation system in order to identify the stable phase in NaCl clearly at each $P$-$T$ condition.

Generated pressures were calculated on the basis of the volume fractions ($V/V_0$) of MgO mixed with NaCl using three equations of state (those proposed by Jamieson, Fritz, and Manghnani,[13] Matsui, Parder, and Leslie,[14] and Speziale, Zha, and Duffy,[15]) because a well-established pressure scale for MgO is not available at present. Comparison of these pressure scales will be discussed later. In the following section, the pressure scale proposed in Ref. 14 will be used tentatively to represent generated pressures.

### III. RESULTS

The phase boundary between $B1$ and $B2$ phases in NaCl over the temperature range from 1150 to 2000 K was determined on the basis of the experimental data obtained in a single run. 93 x-ray diffraction patterns were collected in order to identify the stable phase in NaCl at various $P$-$T$ conditions. In this run, the cell assembly was first compressed to 15 MN at room temperature and pressure estimated at $28.7\pm0.3$ GPa was generated according to the scale in Ref. 14 From there, the temperature was increased slowly and pressure sharply dropped to $24.9\pm0.1$ GPa at 700 K, presumably due to stress relaxation of NaCl.[16] When the temperature reached 1150 K, the first appearance of the $B2$ phase from the single phase of the $B1$ phase was observed at a pressure of 24.5 GPa. At these $P$-$T$ conditions, two kinds of x-ray diffraction patterns were collected; one was collected without press oscillation and the other was collected with press oscillation.

Figure 2 shows a comparison between these two x-ray diffraction patterns. In the pattern obtained without press oscillation, only two peaks of the $B2$ phase, indexed as (111) and (222), were observed; these are minor peaks in the x-ray diffraction patterns obtained in a previous study.[1] In the x-ray diffraction pattern obtained with press oscillation, we observed an intense peak of the $B2$ phase indexed as (110), which is the most intense peak of $B2$ phase.[1] Two other diffraction peaks of the $B2$ phase [those indexed as (111) and (220)] were also observed in this profile. The relative intensities of these peaks are reasonably consistent with those observed in the previous study.[1] However, not all the peaks of the $B2$ phase were observed in the profile obtained using the press-oscillation system, which may be attributed to the restricted range of angular movement in the oscillation of the press ($-4°$ to $7°$), which is not enough to erase the effect of NaCl grain growth at this temperature. However, the press-oscillation system helped us to identify the stable phase ($B2$ phase) at these $P$-$T$ conditions, because the most intense peak of the $B2$ phase was clearly observed in the diffraction pattern obtained with the press oscillating, whereas this peak was not observed in the diffraction pattern obtained without the press oscillating. Therefore, above this temperature, all the diffraction patterns were collected using the press-oscillation system in order to identify the stable phases in NaCl ($B1$ or $B2$ phase) accurately at each $P$-$T$ condition.

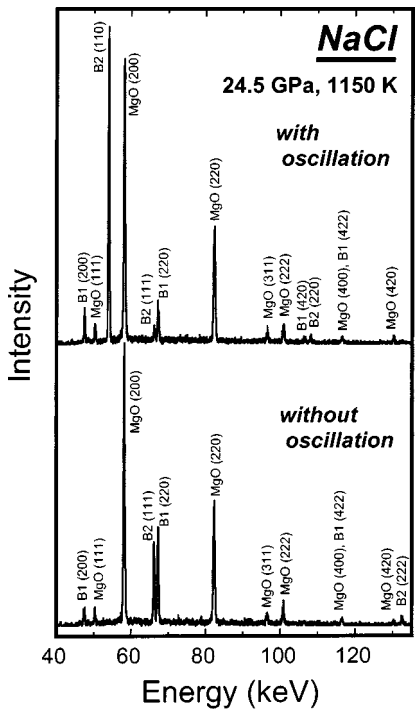


FIG. 2. Comparison between a diffraction pattern collected without press oscillation and that collected with press oscillation. These diffraction patterns were collected at the same $P$-$T$ conditions of 24.7 GPa and 1150 K using the energy-dispersive method with a fixed angle of about 6°. The most intense peak of the $B2$ phase indexed as (110) was observed in the diffraction pattern obtained with the press oscillation, whereas this peak was not observed in that obtained without press oscillation. The press oscillation dramatically reduces the effect of NaCl grain growth at high temperature on diffraction patterns obtained using the energy-dispersive method.

Figure 3 illustrates how the x-ray diffraction pattern changed with increasing and decreasing temperature. At $P$-$T$ conditions of 24.4 GPa and 1000 K, only diffraction peaks of the $B1$ phase were observed [Fig. 3(a)]. When the temperature was increased to 1150 K at a fixed load, the appearance of peaks of the $B2$ phase was observed and as a result, diffraction peaks of both $B1$ and $B2$ phases were present [Fig. 3(b)]. Thus, we regard these $P$-$T$ conditions as corresponding to those of the $B1$ to $B2$ phase transition. After that, the temperature was increased to 1200 K, and complete disappearance of the diffraction peaks of the $B1$ phase was observed [Fig. 3(c)], indicating that the $B2$ phase is stable at these $P$-$T$ conditions. When the temperature was decreased from 1200 to 1150 K, we observed the reappearance of the $B1$ phase [Fig. 3(d)]. Thus, we regard these $P$-$T$ conditions as corresponding to those of the $B2$ to $B1$ phase transition. At 1150 K, we were able to determine the phase transition pressures of the forward ($B1$ to $B2$) and backward ($B2$ to $B1$) transitions; these transition pressures are completely consistent with each other, which strongly indicates that there is no kinetic effect in the forward and backward transitions above 1150 K.

All the experimental data obtained in the present study are summarized in Table I. Pressures calculated using three dif-

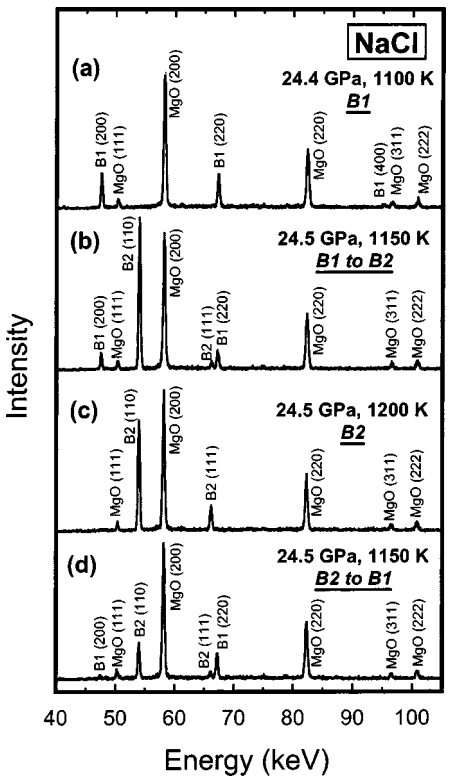


FIG. 3. An example of the change of x-ray diffraction patterns of NaCl with increasing and decreasing temperature at a constant ram load of 15 MN: (a) at 24.4 GPa and 1100 K; (b) $B1$ to $B2$ transition (forward transition) at 24.5 GPa and 1150 K; (c) in the stability field of the $B2$ phase at 24.5 GPa and 1200 K; (d) $B2$ to $B1$ transition (backward transition) at 24.5 and 1150 K.

ferent equations of state of MgO are also listed along with its volume fractions. At temperatures between 1150 and 1600 K, pressures of the forward and backward transitions were determined in the same manner as the measurements at 1150 K. The forward transitions were observed by increasing the temperature at a constant ram-load (data nos. 20, 31, 45, 55, and 64 in Table I), whereas the backward transitions were observed by decreasing temperature at a constant ram load (data no. 24), or by decreasing ram load at a constant temperature (data nos. 28, 41, and 51), which leads to a decrease in pressure at a constant temperature, as suggested in Table I.

At conditions of 1600 K and 22.1 GPa (data no. 64), only the (110) peak of the $B2$ phase was observed along with some diffraction peaks of the $B1$ phase, which we attribute to further grain growth of the $B2$ phase because of the long duration of the heating step near the phase boundary between the $B1$ and $B2$ phases. Then the temperature was suddenly dropped to 700 K within a few seconds and diffraction peaks of the $B1$ phase were observed, the relative intensities of which were reasonably consistent with those of a JCPDS (Joint Committee on Powder Diffraction Standards) card. Since the resultant $P$-$T$ conditions were far from the phase boundary, recrystallization of the $B1$ phase with fine grains may have occurred. After that, temperature was suddenly increased to 1650 K (data no. 65) and a single phase of the $B2$ phase was observed. Immediately after that, the temperature was decreased to 1570 K (data no. 66) and a single phase of the $B1$ phase was observed. Thus, we observed a complete transition from the single phase of $B2$ at 1650 K to that of the $B1$ phase at 1570 K, and we can conclude that the phase boundary lies between these two $P$-$T$ conditions.

After that, temperature was suddenly decreased to 700 K in order to avoid further grain growth of NaCl, and the cell assembly was compressed from 5.75 to 10 MN (data nos. 66–74) at this temperature. At a constant load of 10 MN, the temperature was suddenly increased to 1600 and 1800 K and then suddenly decreased to 1700 K, and complete transitions from one phase to the other were observed, from which we were able to place restrictions on the $P$-$T$ conditions of the phase boundary (data nos. 74–76). In order to place some restrictions on those at temperatures above 1800 K, decompression at 1200 K and the following sudden increases and decreases of temperature were repeated (data nos. 76–91). The method to place restrictions on the $P$-$T$ conditions of the phase boundary at temperatures above 1600 K (i.e., compression and decompression at relatively low temperature, and the following rapid increases and decreases in temperature) is similar to that employed by Katsura *et al.*[17] to determine the postspinel transition in $Mg_2SiO_4$. This method is sometimes effective for restricting a phase boundary especially at high temperature.

The last x-ray diffraction pattern in this experiment was collected at 20.1 GPa and 2100 K (data no. 93). In this profile, no diffraction peaks of either the $B1$ or the $B2$ phase were observed. Only two diffraction peaks of MgO indexed as (200) and (220) were observed, with a weak halo superimposed on these diffraction peaks. Thus, we concluded that NaCl melted at these $P$-$T$ conditions.

Figure 4 shows the phase boundary between the $B1$ and $B2$ phases in NaCl determined in the present study. The horizontal axis represents the pressure calculated using the scale in Ref. 14 At temperatures between 1150 and 1600 K, forward and backward transitions were observed independently. Above 1600 K, some restrictions can be placed by observations of complete transitions from one phase to the other; in this figure, upward and downward arrows represent complete transitions from the $B1$ to the $B2$ phase and those from the $B2$ to the $B1$ phase, respectively. $P$-$T$ conditions where the forward and backward transitions were observed were fitted to a linear function by least-squares regression, and a resultant formula, given by $P\ (\mathrm{GPa}) = 30.6(2) - 0.0053(2)\ T\ (\mathrm{K})$ was derived, which is represented by a the dashed line between the $B1$ and the $B2$ phase in Fig 4. The numbers in parentheses are errors of the fitting. No contradiction is found between this line and the restrictions placed on the phase boundary at temperatures above 1600 K. Therefore, we conclude that this line represents the equilibrium phase boundary between the $B1$ and $B2$ phases in NaCl at temperatures between 1150 and 2000 K.

In addition, liquid NaCl was observed at 20.1 GPa and 2100 K (data no. 93; see Table I). Taking all the experimental data obtained by the present study into consideration, the triple point between $B1$, $B2$, and liquid NaCl would be located at a pressure of about $19.7 \pm 0.5$ GPa and a temperature of about $2050 \pm 50$ K (see Fig. 4).

TABLE I. Experimental conditions and phase present in NaCl. Symbols used: $P_J$, pressures by Jamieson, Fritz, and Manghnani (Ref. 13); $P_M$, pressures by Matsui, Parder, and Leslie (Ref. 14); $P_S$, pressures by Speziale, Zha, and Duffy (Ref. 15). $B1$, only $B1$ phase was observed; $B2$, only $B2$ phase was observed. $B1$-$B2$, appearance of $B2$ phase was observed from $B1$ phase. $B2$-$B1$, appearance of $B1$ phase was observed from $B2$ phase.

| Data no. | Load (MN) | Temp. (K) | MgO | | | | NaCl phase present |
|---|---|---|---|---|---|---|---|
| | | | $V/V_0$ | $P_J$ (GPa) | $P_M$ (GPa) | $P_S$ (GPa) | |
| 9[a] | 0 | 300 | 1.0000(3) | 0.00(04) | 0.00(04) | 0.00(04) | $B1$ |
| 10[a] | 15 | 300 | 0.8717(8) | 28.83(27) | 28.72(26) | 28.94(26) | $B1$ |
| 12[a] | 15 | 570 | 0.8862(6) | 25.81(17) | 26.00(17) | 26.17(17) | $B1$ |
| 13[a] | 15 | 700 | 0.8929(5) | 24.57(14) | 24.90(14) | 25.10(14) | $B1$ |
| 14[a] | 15 | 800 | 0.8963(3) | 24.18(09) | 24.59(09) | 24.81(08) | $B1$ |
| 15[a] | 15 | 900 | 0.8996(3) | 23.84(09) | 24.34(09) | 24.56(08) | $B1$ |
| 17[a] | 15 | 980 | 0.9008(4) | 23.95(11) | 24.52(11) | 24.76(11) | $B1$ |
| 18[a] | 15 | 1100 | 0.9041(3) | 23.79(09) | 24.44(09) | 24.67(08) | $B1$ |
| 19[a] | 15 | 1150 | 0.9049(4) | 23.86(12) | 24.56(12) | 24.79(11) | $B1$-$B2$ |
| 20 | 15 | 1150 | 0.9051(3) | 23.81(08) | 24.51(08) | 24.74(08) | $B1$-$B2$ |
| 23 | 15 | 1200 | 0.9064(4) | 23.75(10) | 24.49(10) | 24.73(10) | $B2$ |
| 24 | 15 | 1150 | 0.9051(4) | 23.81(11) | 24.51(11) | 24.74(11) | $B2$-$B1$ |
| 25 | 15 | 1200 | 0.9067(4) | 23.68(10) | 24.41(10) | 24.65(10) | $B2$ |
| 28 | 11 | 1200 | 0.9076(4) | 23.46(10) | 24.20(10) | 24.42(10) | $B2$-$B1$ |
| 30 | 11 | 1150 | 0.9060(3) | 23.57(07) | 24.27(07) | 24.51(08) | $B1$ |
| 31 | 11 | 1200 | 0.9077(3) | 23.42(09) | 24.16(09) | 24.39(08) | $B1$-$B2$ |
| 35 | 11 | 1300 | 0.9104(3) | 23.33(08) | 24.14(08) | 24.36(08) | $B2$ |
| 41 | 9 | 1300 | 0.9122(4) | 22.88(10) | 23.70(10) | 23.90(10) | $B2$-$B1$ |
| 43 | 9 | 1200 | 0.9096(4) | 22.93(10) | 23.67(10) | 23.90(10) | $B1$ |
| 45 | 9 | 1300 | 0.9118(5) | 22.97(12) | 23.79(12) | 24.00(13) | $B1$-$B2$ |
| 47 | 9 | 1400 | 0.9152(3) | 22.71(08) | 23.61(08) | 23.81(07) | $B2$ |
| 51 | 7 | 1400 | 0.9171(5) | 22.24(11) | 23.14(11) | 23.34(12) | $B2$-$B1$ |
| 52 | 7 | 1350 | 0.9161(3) | 22.20(08) | 23.07(08) | 23.26(07) | $B1$ |
| 55 | 7 | 1500 | 0.9215(3) | 21.80(06) | 22.77(06) | 22.93(07) | $B1$-$B2$ |
| 56 | 7 | 1550 | 0.9222(4) | 21.94(09) | 22.95(09) | 23.09(10) | $B2$ |
| 63 | 5.75 | 1550 | 0.9250(6) | 21.27(13) | 22.28(13) | 22.42(14) | $B1$ |
| 64 | 5.75 | 1600 | 0.9274(7) | 21.00(15) | 22.05(15) | 22.19(16) | $B1$-$B2$ |
| 65 | 5.75 | 1650 | 0.9299(5) | 20.75(12) | 21.84(11) | 21.94(12) | $B2$ |
| 66 | 5.75 | 1570 | 0.9270(7) | 20.92(16) | 21.95(16) | 22.08(16) | $B1$ |
| 74 | 10 | 1600 | 0.9325(6) | 19.85(13) | 20.90(13) | 21.01(14) | $B1$ |
| 75 | 10 | 1800 | 0.9368(5) | 20.12(10) | 21.31(10) | 21.36(11) | $B2$ |
| 76 | 10 | 1700 | 0.9337(6) | 20.19(13) | 21.30(13) | 21.40(14) | $B1$ |
| 81 | 6.75 | 1700 | 0.9357(5) | 19.75(10) | 20.86(10) | 20.95(11) | $B1$ |
| 83 | 6.75 | 1850 | 0.9397(3) | 19.79(07) | 21.01(07) | 21.05(07) | $B2$ |
| 86 | 6 | 1950 | 0.9429(4) | 19.72(08) | 21.00(08) | 21.02(09) | $B2$ |
| 87 | 6 | 1800 | 0.9391(4) | 19.62(09) | 20.80(09) | 20.85(09) | $B1$ |
| 90 | 5.5 | 2000 | 0.9471(7) | 19.15(15) | 20.46(15) | 20.46(15) | $B2$ |
| 91 | 5.5 | 1900 | 0.9450(5) | 18.97(10) | 20.22(10) | 20.24(11) | $B1$ |
| 93 | 5.0 | 2100 | 0.9522(2) | 18.73(04) | 20.09(05) | 20.10(04) | Liq. |

[a]collected without press oscillation.

## IV. DISCUSSION

### A. Comparison with previous studies

The phase boundary between $B1$ and $B2$ phases in NaCl determined in the present study is compared with those determined in previous studies in Fig. 5. The phase boundary in the present study is extrapolated to 300 K and the transition pressure at this temperature is estimated to be 29.3 GPa, which is close to or slightly smaller than the $B1$ to $B2$ phase transition pressure at 300 K determined by previous studies using the diamond anvil cell[1,2] and Kawai-type apparatus with sintered diamond anvils.[3]

The Clapeyron slope determined in the present study is $-5.3$ MPa/K, which is different from that determined by Li

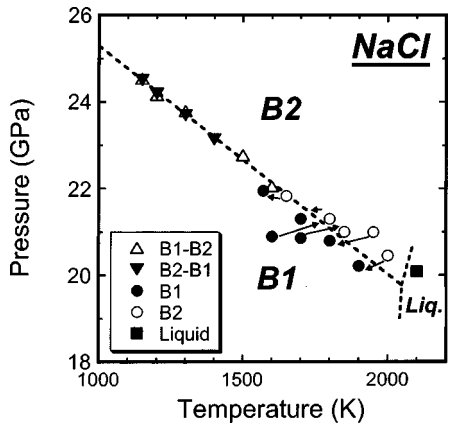


FIG. 4. The equilibrium phase boundary between $B1$ and $B2$ phases in NaCl determined in the present study (a dashed line between $B1$ and $B2$ phases). Open and closed triangles represent $P$-$T$ conditions where the $B1$ to $B2$ (forward) and $B2$ to $B1$ (backward) transitions were observed, respectively. Open and closed circles represent $P$-$T$ conditions where single phases of $B1$ and $B2$ were observed, respectively. At $P$-$T$ conditions of 20.1 GPa and 2100 K, liquid NaCl was observed (a solid square). Upward and downward arrows represent direct transitions from the $B1$ to $B2$ phase and those from the $B2$ to $B1$ phase, respectively (see text). According to the present experimental results, the triple point among $B1$, $B2$, and liquid NaCl would be located at a pressure of $19.7 \pm 0.5$ GPa and at a temperature of $2050 \pm 50$ K.

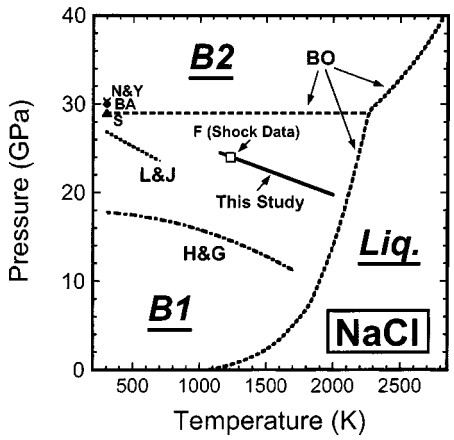


FIG. 5. Comparison of the phase boundary between $B1$ and $B2$ phases in NaCl with those of the previous studies. The closed circle and triangle represent the $B1$ to $B2$ transition pressure at room temperature determined by Bassett *et al.* (Ref. 1) (BA) and by Sato-Sorensen (Ref. 2) (S), respectively, using the diamond anvil cell, whereas the cross represents that determined by Nishiyama and Yagi (Ref. 3) (N&Y) using the Kawai-type apparatus with sintered diamond anvils. Li and Jeanloz (Ref. 9) (L&J) determined this phase boundary at temperatures up to 673 K using an externally heated diamond anvil cell (the dotted line) and Hemley and Gordon (Ref. 20) (H&G) studied this phase boundary theoretically (the dash-dotted line). Beohler, Ross, and Boercker (Ref. 10) (BO) measured melting temperatures of NaCl at pressures up to 91 GPa and estimated $P$-$T$ conditions where this phase boundary exists (see text) (the dashed line). The open square represents the $P$-$T$ conditions where this transition was observed in a shock compression study by Fritz *et al.* (Ref. 8) (F).

and Jeanloz[9] ($-8.6$ MPa/K) using an externally heated diamond anvil cell. They determined transition pressures of the forward and the backward transitions independently at temperatures up to 673 K and deduced that the equilibrium transition pressure at a given temperature is the average of the forward and backward transition pressure. They judged the phase transition by the visual observation using a transmitted-light microscope; the $B1$ and $B2$ phases coexisted with each other because of the pressure gradient in a diamond anvil cell, and they were able to distinguish one phase from the other because of the mismatch in refractive indices of these two phases. Pressure was measured using the ruby fluorescence technique[18] with temperature correction,[19] and the phase-transition pressure at a given $P$-$T$ condition was determined using a ruby grain that existed on the boundary between the two phases.

In contrast, in the present study the stable phase of NaCl at a given $P$-$T$ condition was directly determined using the *in situ* x-ray observation, and the $P$-$T$ conditions where the forward and backward transitions occur fall on a straight line at temperatures between 1150 and 1600 K, which indicate that the temperature range of the present study is high enough to eliminate the kinetic effect of the forward and backward transitions and to determine the equilibrium phase-transition pressure precisely (see Fig. 4). Therefore the method used to identify the stable phase in the present study, as well as the experimental temperatures, is different from that of the study by Li and Jeanloz,[9] which may account for the difference in the Clapeyron slopes determined in these two studies.

In addition, there is a difference in the method used to measure pressure in these two studies. In the present study, pressures were determined on the basis of volume fraction data for MgO mixed with NaCl using the equations of state for MgO, whereas in the study of Li and Jeanloz,[9] pressures were determined using the ruby fluorescence technique[18] with temperature correction.[19] The accuracy of pressure determination at high temperature clearly and seriously affects the value of the Clapeyron slope of this phase boundary.

Hemley and Gordon[20] have also determined this phase boundary theoretically. They studied the properties of NaF and NaCl at high pressures in both the $B1$ and $B2$ phases with an improved electron-gas model and deduced the phase boundaries between these two phases in both materials from the resultant physical properties. In the case of NaF, the phase transition pressure at 300 K was determined to be about 37 GPa, whereas Sato-Sorensen[2] and Yagi, Suzuki, and S. Akimoto[21] determined the transition pressure experimentally using diamond anvil cells to be $23 \pm 3$ and $27 \pm 1$ GPa, respectively, which are far different from those determined theoretically. In the case of NaCl, the theoretically determined phase transition pressure at 300 K is also inconsistent with those determined by the experiments (see Fig. 5). However, the Clapeyron slope of the theoretically determined phase boundary seems to be close to that determined in the present study at temperatures above about 1000 K.

Boehler, Ross, and Boercker[10] measured the melting temperature of NaCl at various pressures up to 91 GPa using a laser-heated diamond anvil cell. The $P$-$T$ conditions where liquid was observed in the present study (i.e., 20.1 GPa and 2100 K) are consistent with their melting curve (e.g., $T_m = 2091 \pm 120$ K at 21.3 GPa). They observed a discontinuous increase in the slope of the melting curve at about 29 GPa ($T_m \sim 2250$ K) and considered that there was a triple point between $B1$, $B2$, and liquid NaCl at around these $P$-$T$ conditions. They connected these $P$-$T$ conditions with those at 29 GPa and 300 K (where the $B1$ to $B2$ phase transition was observed by previous studies[1–3]) and suggested that the slope of the phase boundary between the $B1$ and the $B2$ phases in NaCl is close to zero (see Fig. 5). However, all the experimental studies to determine the $B1$-$B2$ phase boundary directly, including a study using shock compression,[8] have demonstrated that this phase boundary has a negative Clapeyron slope. Since the melting temperatures measured in Ref. 10 have an experimental error of about $\pm 100$ K, rigid restrictions cannot be placed on the $P$-$T$ conditions of the triple point.

Bassett *et al.*[1] made a systematic comparison of the Clapeyron slopes for four alkali-metal chlorides (CsCl, RbCl, KCl, and NaCl). According to thermodynamic relations, the entropy change ($\Delta S$) at the phase-transition pressure has a linear relationship with $\Delta V/V_{01}$ for the alkali-metal chlorides (see Ref. 1); $\Delta V$ is the volume change at the phase transition pressure, and $V_{01}$ is the volume of the $B1$ phase at ambient conditions. They estimated the Clapeyron slope ($dP/dT$) of the $B1$-$B2$ phase boundary in NaCl by connecting the transition pressure ($30 \pm 1$ GPa) that they determined at room temperature to that determined by shock compression method[8] (24 GPa at 1231 K). The resultant $dP/dT$ is $-6.4$ MPa/K, which is close to that determined in the present study. $\Delta S$ of NaCl can be calculated using the Clausius-Clapeyron equation ($dP/dT = \Delta S/\Delta V$) and $\Delta V$ was determined on the basis of their measurements at room temperature. Bassett *et al.*[1] also calculated $\Delta S$ and $\Delta V/V_{01}$ for the other three alkali-metal chlorides using thermodynamic parameters for these materials and found that a highly linear relationship between $\Delta V/V_{01}$ vs $\Delta S$. The fact that the precisely determined Clapeyron slope in the present study is approximately consistent with the thermodynamically reasonable one determined by Bassett *et al.*[1] indicates that these values for the Clapeyron slopes are highly reliable.

### B. Comparison of pressure scales of MgO

In order to assess the reliablility of the phase boundary determined in the present study, the three MgO pressure scales[13–15] used in the present study are compared with each other on the basis of the volume fraction data obtained in this study. In this comparison, the volume fraction obtained at 20.1 GPa and 2100 K (data no. 93) is excluded because the unit-cell volume of MgO at these conditions was calculated using only two diffraction peaks, (200) and (220). At all the other $P$-$T$ conditions, the unit-cell volumes were calculated using five diffraction peaks, (111), (200), (220), (311), and (222). In Fig. 6, the horizontal axis represents pressure calculated using the scale in Ref. 14, which was tentatively used in this study, and the vertical axis represents pressure calculated using the other two pressure scales.[13,15] Since the data points in this figure are calculated from the volume-fraction data collected in the present study, pressure values at various temperatures are included. X-ray diffraction data were obtained along the phase boundary between the $B1$ and the $B2$ phases in NaCl, which has a negative Clapeyron slope. Thus, the data points at around 29 GPa are those at 300 K, and the data points at lower pressures are those at higher temperatures (see Table I and Fig. 4). Pressures calculated using the scale in Ref. 17 show a great deal of consistency with those from the scale in Ref. 14. On the other hand, pressures from the scale in Ref. 13 are lower than those from the Ref. 14 scale by about 1 GPa, especially at high temperatures (see Fig. 6 and Table I).

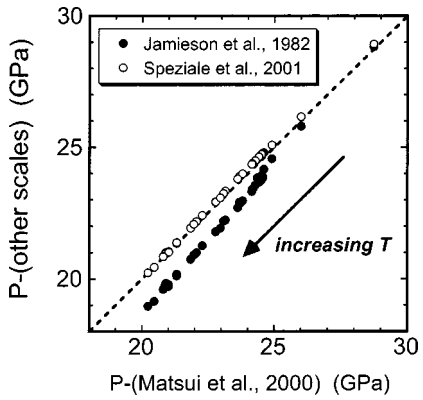


FIG. 6. Comparison of pressure scales of MgO. The horizontal axis represents pressures calculated using the Matsui-Parder-Leslie scale (Ref. 14) whereas the vertical one represents pressures calculated using the Jamieson-Fritz-Manghnani (Ref. 13) and Speziale-Zha-Duffy (Ref. 15) scales. Pressures of the vertical scales show a great deal of consistency with each other. Pressures of the horizontal scale are lower than those of the other two scales (see text).

A $P$-$V$-$T$ relation for MgO proposed by Matsui, Parder, and Leslie[14] was determined using the molecular dynamics method with quantum corrections, not using any equation of state model. Parameters for the interionic potential were derived to reproduce experimental data. The experimental data used for the references are as follows: thermal expansion at room pressure, Dubrovinsky and Saxena;[22] compression at room temperature, Fei;[23] isothermal elastic moduli and their temperature derivatives, Isaak, Anderson, and Goto;[24] pressure derivatives of elastic constants, four studies.[25]

On the other hand, Speziale, Zha, and Duffy[15] carried out quasihydrostatic compression experiments on MgO and proposed a Birch-Murnaghan-Debye thermal equation of state in combination with experimental data that had been reported to that date. They used thermal expansion data at room pressure collected by Fiquet, Richet, and Montagnac,[26] compression data at room temperature by Fei,[23] those at high-pressure and temperature conditions by Utsumi, Weidner, and Liebermann[27] and Dewaele,[28] and shock compression data by Svendsen and Ahrens.[29] The scales of Refs. 14 and 15 are based on the same data of compression at room temperature by Fei.[23] In addition, thermal expansion data at

room pressure obtained by Dubrovinsky and Saxena,[22] which was employed to construct the Ref. 14 scale, is highly consistent with those obtained by Fiquet, Richet, and Montagnac,[26] which was used to construct the Ref. 15 scale. Therefore, both scales in Refs. 14 and 15 are based on virtually the same experimental data for room-temperature compression and thermal expansion at room pressure. Thus, these scales are closely related, rather than completely distinguishable. Hence, the consistency between these scales cannot be used to ensure the credibility of these scales. Nevertheless, we conclude that these two scales are the most reliable in terms of MgO pressure scales at present, because the Ref. 14 scale shows great consistency with a pressure scale developed by Cohen,[30] using a molecular dynamics simulation based on nonempirical interatomic potential over a wide range of pressures and temperatures.[31]

On the other hand, the inaccuracy of the Ref. 13 scale has already been discussed.[14] Some key parameters employed to construct this scale have some serious errors and the harmonic Debye model that was employed in this scale is not appropriate for MgO, especially at high temperature. In order to construct a more reliable pressure scale for MgO, further studies are needed, including simultaneous measurements of acoustic velocities and the $P$-$V$-$T$ relation of MgO and comparison with other pressure scales, such as NaCl, Au, and Pt scales over a wide range of pressures and temperatures.

## ACKNOWLEDGMENTS

We thank T. Irifune, R. P. Rapp, T. Inoue, D. Yamazaki, T. Yagi, Y. Wang, T. Uchida, M. Matsui, S. Sakamoto, and M. Isshiki for conclusive comments and discussion. We also thank T. Sanehira for technical assistance in the preparation of experiments. *In situ* x-ray diffraction experiments were carried out at SPring-8 (Proposal No. 2002B0044-CD2-np and 2003A0088-ND2-np). This work was partly supported by the Japan Society for the Promotion of Science for Young Scientists to N.N.

*Author to whom correspondence should be addressed. Email address: nisiyama@sci.ehime-u.ac.jp

[1] W. A. Bassett, T. Takahashi, H.-K. Mao, and J. S. Weaver, J. Appl. Phys. **39**, 319 (1968).
[2] Y. Sato-Sorensen, J. Geophys. Res. **88**, 3543 (1983).
[3] N. Nishiyama and T. Yagi, J. Geophys. Res. **108**, 10.1029/2002JB002216 (2003).
[4] D. L. Decker, J. Appl. Phys. **42**, 3239 (1971).
[5] F. Birch, J. Geophys. Res. **91**, 4949 (1986).
[6] J. M. Brown, J. Appl. Phys. **86**, 5801 (1999).
[7] B. J. Alder, in *Solids Under Pressure*, edited by W. Paul and D. M. Warschauer (McGraw-Hill, New York, 1963), p. 478.
[8] N. Fritz, S. P. Marsh, W. J. Carter, and R. G. McQueen, in *Accurate Characterization of the High-Pressure Environment*, Natl. Bur. Stand. (U.S.) Spec. Pub. No. 326, edited by E. C. Lloyd (U. S. GPO, Washington, D. C., 1968), p. 201.
[9] X. Li and R. Jeanloz, Phys. Rev. B **36**, 474 (1987).
[10] R. Boehler, M. Ross, and D. B. Boercker, Phys. Rev. Lett. **78**, 4589 (1997).
[11] T. Katsura, K. Funakoshi, A. Kubo, N. Nishiyama, Y. Tange, Y. Sueda, T. Kubo, and W. Utsumi, Phys. Earth Planet. Inter. (to be published).
[12] K. Kuroda, T. Irifune, T. Inoue, N. Nishiyama, M. Miyashita, K. Funakoshi, W. Utsumi, Phys. Chem. Miner. **27**, 523 (2000).
[13] J. C. Jamieson, J. N. Fritz, and M. H. Manghnani, in *High-Pressure Research in Geophysics*, edited by S. Akimoto and M. H. Manghnani (Center for Academic Publications, Tokyo, 1982), p. 27.
[14] M. Matsui, S. C. Parder, and M. Leslie, Am. Mineral. **85**, 312 (2000).
[15] S. Speziale, C.-S. Zha, and T. S. Duffy, J. Geophys. Res. **106**, 515 (2001).
[16] Y. Wang, D. J. Weidner, and Y. Meng, in *Properties of Earth and Planetary Materials at High Pressure and Temperature*, edited by M. H. Manghnani and T. Yagi, (American Geophys. Union, Washington, D. C., 1998), p. 356.
[17] T. Katsura, H. Yamada, T. Shinmei, A. Kubo, S. Ono, M. Kanzaki, A. Yoneda, M. J. Walter, E. Ito, S. Urakawa, K. Funakoshi, W. Utsumi, Phys. Earth Planet. Inter. **136**, 11 (2003).
[18] H.-K. Mao, P. M. Bell, J. W. Shaner, and D. J. Steinberg, J. Appl. Phys. **49**, 3276 (1978).
[19] R. C. Powell, B. DiBartolo, B. Birang, and C. S. Naiman, J. Appl. Phys. **37**, 4973 (1966).
[20] R. J. Hemley and R. G. Gordon, J. Geophys. Res. **90**, 7803 (1985).
[21] T. Yagi, T. Suzuki, and S. Akimoto, J. Phys. Chem. Solids **44**, 135 (1983).
[22] L. S. Dubrovinsky and S. K. Saxena, Phys. Chem. Miner. **24**, 547 (1997).
[23] Y. Fei, Am. Mineral. **84**, 272 (1999).
[24] D. G. Isaak, O. L. Anderson, and T. Goto, Phys. Chem. Miner. **16**, 704 (1989).
[25] Z. P. Chang and G. R. Barsch, J. Geophys. Res. **74**, 3291 (1969); H. Spetzler, *ibid.* **75**, 2073 (1970); I. Jackson, and H. Niesler, in *High-Pressure Research in Geophysics* (Ref. 13), p. 93; A. Yoneda, J. Phys. Earth **38**, 19 (1990).
[26] G. Fiquet, P. Richet, and G. Montagnac, Phys. Chem. Miner. **27**, 103 (1999).
[27] W. Utsumi, D. J. Weidner, and R. C. Liebermann, in *Properties of Earth and Planetary Materials at High Pressure and Temperature* (Ref. 16), p. 327.
[28] A. Dewaele, G. Fiquet, D. Andrault, and D. Hausermann, J. Geophys. Res. **105**, 2869 (2000).
[29] B. Svendsen and T. J. Ahrens, Geophys. J. R. Astron. Soc. **91**, 667 (1987).
[30] R. E. Cohen, in *Physics Meets Mineralogy*, edited by H. Aoki, Y. Syono, and R. J. Hemley (Cambridge Univ. Press, Cambridge, 2000), p. 95.
[31] M. Matsui and N. Nishiyama, Geophys. Res. Lett. **29**, 1029/2001GL014161 (2002).